Preprint. To read the published version go to the following link:
https://doi.org/10.1016/j.nimb.2020.05.019

Non-destructive identification of surface enrichment and trace element fractionation in ancient silver coins

Mahir Hrnjić[1*], Graham Adrian Hagen-Peter[1, 2, 3], Thomas Birch[1, 2], Gry Hoffmann Barfod[1, 2], Søren Michael Sindbæk[1], Charles Edward Lesher[1, 2]

[1] Centre for Urban Network Evolutions, Department of Archaeology and Heritage Studies, School of Culture and Society, Aarhus University, 8000 Aarhus, Denmark

[2] The Aarhus Geochemistry and Isotope Research (AGiR) Platform, Institute for Geoscience, Faculty of Science and Technology, Aarhus University, 8000 Aarhus, Denmark

[3] Geological Survey of Norway, 7040 Trondheim, Norway

ORCID iD:

Mahir Hrnjić https://orcid.org/0000-0001-6359-7113

Graham Adrian Hagen-Peter https://orcid.org/0000-0003-3499-3816

Thomas Birch https://orcid.org/0000-0002-4568-9767

Gry Hoffmann Barfod https://orcid.org/0000-0002-7000-0757

Søren Michael Sindbæk https://orcid.org/0000-0002-1254-1256

Charles Edward Lesher https://orcid.org/0000-0003-4033-4809

*Corresponding author information

Phone: +45 4234 2070

Email: mahir.hrnjic@cas.au.dk

Abstract

A common issue in non-destructive surface analysis of historical silver coins is depletion of Cu from the near-surface areas, which in turn results in higher Ag content at a coin's surface. This paper reports a non-destructive analytical strategy using μXRF for identification of Ag and Cu surface enrichments and depletions by comparing peak intensity ratios of Ag Kα/Ag Lα, Cu Kα/Ag Kα and Cu Lα/Ag Lα for coins and Ag-Cu standards of similar composition. Our characterization of coins from different contexts and chronologies shows that a multi-standard approach provides the most reliable identification of surface enrichment of Ag and depletion of Cu. Coins possessing Ag surface enrichment were further analysed with LA-ICP-MS to determine any differences in trace element composition between the cores and surface of the coins. We show that the near-surface regions of these coins are enriched in Au and depleted in Co, Ni, As, and Pt relative to their cores. These systematics allow for a more robust assessment of the degree of silver coin surface alteration critically important in measuring the original composition of historical silver coins.

Keywords

Silver coins, silver surface enrichment, trace elements, μXRF, LA-ICP-MS

1. Introduction

Silver played an important role as an exchange medium in Ancient and Medieval pre-monetary and monetary economies. Coins therefore are useful for ~~d~~developing a better understanding of political history, economy, and development of commerce. Archaeometric studies of silver coins reveal information regarding the interactions, technology, and economy at particular points in history [1–3]. Since authentic historical coins are limited and rare items, the chemical analysis of the objects should ideally preserve the integrity of a coin, while giving reliable analytical information about its composition. However, surface treatments, conservation actions as well as environmental and galvanic corrosion have been shown to alter the surface composition of a silver coin and thus affect the reliability of non-invasive surface analysis techniques [2,4–13]. The condition of preservation of coins may be affected by exposure to groundwater, soils and/or air due to the difference in electrode potential between Ag and Cu in a two-phase alloy, which may cause the Cu-rich phase to leach to the surface and corrode when exposed to the environmental influences. To the contrary, surface Ag enrichment was sometimes intentionally produced, the most common methods being exposing Ag-Cu coins to high temperatures for a prolong period of time in an oxidizing atmosphere [2,14,15] or blanching the coins in vinegar or citric acid [16,17]. Cu from near-surface areas can be oxidized and form primary corrosion products such as cuprite (Cu_2O) and tenorite (CuO). Subsequently removing this corrosion produced an Ag-rich coin surfaces depleted in Cu. Such production methods are referred in literature as depletion silvering, while silver surface enrichment (SSE) is used as a general term to described Ag enrichment, whether it be intentional or post-depositional. In cases where coins exhibit such phenomena, surface analysis by non-invasive techniques lead to inaccurate elemental concentrations of the major constituents such as Ag and Cu [6]. The surface enrichment in historical coins has been studied extensively with a variety of destructive and non-destructive archaeometrical techniques. An overview of surface enrichment research and how it has affected the study of Roman silver coins can be found in Butcher & Ponting [2]. During the past two decades, a number of studies were dedicated to understand the formation of enrichment, and its effects on the analytical results in coins studied using non-destructive techniques [4–6,9,11–15,18–21].

This study aims to assess the application of XRF Ag Kα/Ag Lα peak intensities method in detecting near-surface enrichment in historical silver coins by pairing coins and different standards with varying content of Ag and Cu. Furthermore, a new method for non-destructive identification of enrichment that combines Cu Kα/Ag Kα and Cu Lα/Ag Lα is introduced. Besides Ag and Cu, LA-ICP-MS analysis of coins' core and enriched areas are performed to monitor the effect of surface enrichment on the behaviour of minor and trace elements commonly present in historical silver.

1. 1 Background

Several studies have examined the reliability of non-destructive spectroscopic analysis of silver coins. Linke et al. [13,18–20] present a non-invasive method for surface enrichment identification using the X-ray Fluorescence (XRF) technique. The study used the ratio of peak intensities of Ag Kα and Ag Lα to determine the presence or absence of silver enrichment by comparing values obtained from different information depths of Ag-Cu coins with a standard of similar composition. Other non-destructive analytical methods such as NAA, XRF, EDXS, PGAA and PIXE/PIGE have been used to retrieve the qualitative and quantitative composition from varying information depths in coins [20,22–27]. For instance, Klockenkämper et al. [12] studied Roman imperial coins with WDXRF and EPMA-EDS to compare the composition of silver coins at 30 µm and 3 µm depths. For analytical methods based on x-ray spectroscopy, the information depth depends on several factors including the energy of the primary incident radiation, absorption coefficient, energy of secondary x-rays, atmosphere, and matrix composition; thus making it dependent on Beer-Lambert law [28]. The secondary radiation produced is relatively weak, and it further changes depending of the matrix in the sample. The main characteristic x-rays for Ag are the Kα and Lα lines that emit fluorescence with different photon energies and thus come from different depths of a matrix.

Stern was first to suggest that Ag Kα and Ag Lα peak intensities can theoretically be used to assess the difference between the surface and bulk composition of a coin [29]. As seen in Figure 1, for a homogenous sample both Ag Kα and Ag Lα interact with a matrix in the same manner despite the Ag Lα radiation (energy 3.0 keV) mostly originating from a depth of up to 2 µm, while the higher energy Ag Kα radiation (energy 22.2 keV) reaches up to 100 µm in a 80 wt. % Ag – 20 wt. % Cu matrix composition [18]. The information depths of Ag Kα and Ag Lα decrease with the increase of Cu content in an alloy. For objects exhibiting surface enrichment, the Ag Lα will derive from the shallow Ag-rich matrix, while Ag Kα will also interact with the deeper Cu-rich matrix, hence the peak intensity of Ag Kα will attenuate. By calculating the ratio of Ag Kα/Ag Lα intensities, it is possible to obtain information on the degree of depletion once the ratio is compared with the Ag Kα/Ag Lα ratio for a non-corroded standard of a similar composition. The difference between the ratios obtained for the enriched surface of a coin and the standard describe the degree of Cu depletion. Besides studies done by Linke et al., this proposed method has been applied in only a small number of studies [9,30,31].

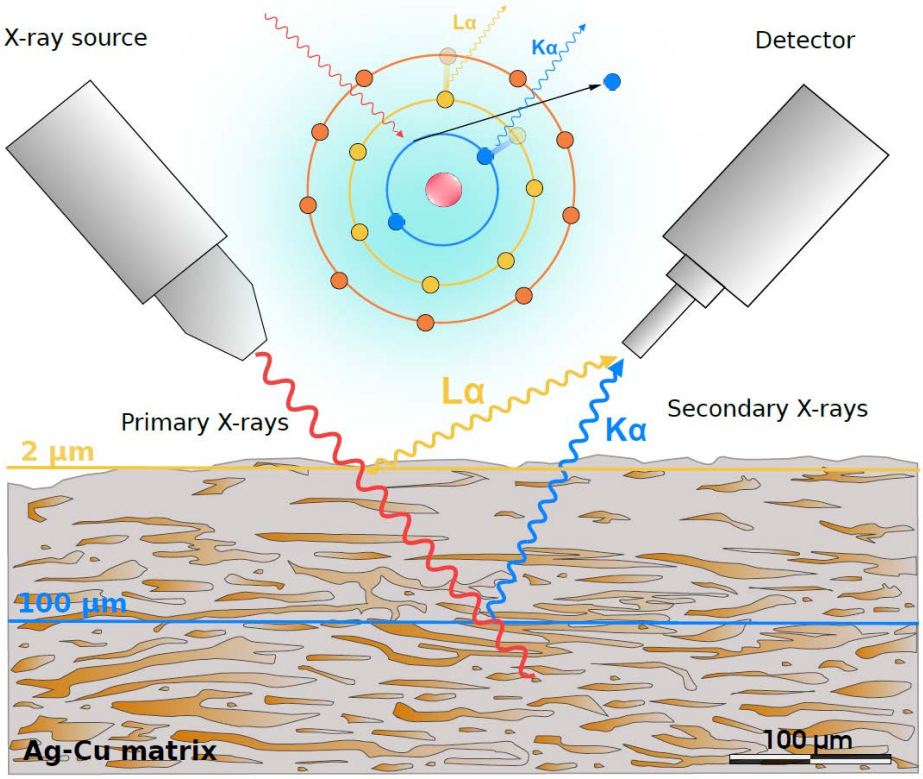

Figure 1. Schematic illustration showing the XRF information depth of Ag Kα and Ag Lα lines in 80 wt. % Ag – 20 wt. % Cu matrix for a Ag enriched coin. Kα radiation derives from the depth of c. 100 µm, while lower energy Lα radiation results from the depth of c. 2 µm. Orange areas = Cu-rich phase, grey matrix = Ag-rich phase.

Besides the major alloy components, minor and trace elements in Ag coins yield critical information about the type and provenance of Ag ores, extraction technology (e.g. cupellation), and metals used in alloying [23,32]. Important tracers for silver provenance include Au and Bi, but due to the often similar composition of silver-producing ores and the effect of trace element fractionation, combining these with lead isotope analysis is more powerful [32,33]. Au/Bi ratios can be useful in distinguishing coins from different sources of silver [30]. However, experiments have demonstrated that whereas the content of Au does not change significantly after smelting and cupellation, Bi follows Pb concentrations by gradually decreasing after each cycle of cupellation, though it is rarely completely removed [34,35]. Experiments using LA-ICP-MS depth profile analysis on medieval silver coins with SSE show a decrease in Au with depth, while Bi and Pb concentrations remain constant [9]. Large differences in the surface enrichment thus may influence the ability to identify different silver groups and a quick and non-destructive screening method such as XRF holds great potential for studying the fineness of silver coins. Such a method can be used to identify

potential outliers in larger studies and would allow researchers to identify optimal analytical and sampling strategies for obtaining reliable chemical composition of silver coins.

A fundamental component of the Ag Kα/Ag Lα method is the selection of an appropriate standard. The majority of historical silver coins were produced with a degree of standardization and with this in mind, the optimal standard will have a similar composition to the original composition of the silver coins. Coins that exhibit surface enrichment can have significantly different Ag and Cu concentrations, hence the original composition of the core of a coin can be difficult to determine with non-destructive analytical techniques. In such cases, choosing a standard with a similar composition as the historical coins can be difficult, unless the core composition of coins is determined beforehand with another technique.

2. Materials and methods

Our study was performed on 12 historical silver-copper alloyed coins (7 Roman denarii, 3 Sassanid coins and 2 early Islamic coins) acquired from a private collector (Table 2). Coins with different chronologies, provenance and composition were used in order to explore the tendency of different types of coins to exhibit silver surface enrichment, as well as to note the efficiency of Ag Kα and Ag Lα method on coins with varying composition. From the 12 coins, 10 were sampled with a jewellery saw on the rim of the coin to obtain a section perpendicular to the flat coin without damaging the relief. These were mounted in epoxy resin, ground with silicon carbide paper with progressively finer grit sizes (180, 220, 550, 1000) and polished on a surface coated with increasingly finer diamond spray (6 µm, 3 µm, 1 µm, ¼ µm). After each grinding and polishing steps, samples were cleaned in an ultrasonic bath for the duration of 5 sec.

For all measurements, a number of Ag-Cu standards with different composition were used. The reference materials (RMs) were acquired from MBH Analytical Ltd. The composition of standards 133X AGA1 A, 133X AGA2 A, 133X AGA3 A and 131X AGP1 B are given in Table 1. Previous studies that dealt with archaeometric analysis of Roman, Sassanid and Islamic coins [2,36,37] show a wide range of silver compositions, which is why a range of standards are needed.

2. 1 Micro X-ray fluorescence (µ-XRF)

We used the benchtop Bruker M4 Tornado µ-XRF for all measurements. The Bruker M4 Tornado operates with a Rh target x-ray tube at a maximum power of 30 W and polycapillary optics that yield a spot size of 20 µm. Analyses are made using the area mapping mode with a voltage of 50kV and tube current of 600 µA in a near-vacuum condition (20 mbar) enabled by a pressure-controlled diaphragm pump. X-rays are detected with the 60 mm^2 XFlash® dual silicon-drift detector system and data is processed using M4 Tornado analysis software 1.5.

In order to validate the reliability of the Ag Kα/Ag Lα method for identification of SSE, cross-sections of 10 coins were analyzed with the purpose of determining changes in Ag and Cu concentrations from surface to core illustrated by the multi-elemental maps in Figure 2. Due to differences in coin-thickness, analyses or mapping varied in area size and duration (10 to 20 min) with a fix step size of 20 µm and dwell time of 10 ms/pixel. The surface areas of coins and standards were also analysed in order to determine Ag Kα and Ag Lα intensity ratios. For this purpose, the selected area for analysis was 6.7x7.0 mm, with a step size of 30 µm (spatial resolution 233x233 pixels) for 15 min with a dwell time 10 ms/pixel. Ag Kα/Ag Lα were obtained by analysing every standard five times. After producing the Ag Kα/Ag Lα intensity ratios of coins and standards, the percent deviation of values was calculated from the ratios obtained from different standards. Cu Kα and Cu Lα were also measured in the effort to explore the possibility to account for the presence of corrosion on the surface of coins. Detailed XRF intensity peak measurements are reported in Supplement 1. As shown in Table 1, Ag is measured in all standards to determine the reproducibility of the instrument, which deemed satisfactory for the present purpose.

Table 1. Composition and Ag Kα/Ag Lα peak intensities ratios determined by µ-XRF for MBH analytical standards.

Ag (wt%)					
RM	Ag*	Measured			AgK/AgL***
		Mean	SD	% error**	
133X AGA1 A	77.37	74.14	0.54	4.17	0.1045
133X AGA2 A	86.97	85.92	1.01	1.21	0.1053
133X AGA3 A	90.53	91.06	0.25	0.58	0.1007
131X AGP1 B	99.34	97.81	0.53	1.54	0.0943

* The amount calculated after deducting the content of all other reported elements from the total weight of the standard.

** Percentage error of the mean Ag concentrations based on 5 replicate analyses of each standard.

*** The peak intensities of AgK and AgL line are measured as cps/eV.

2. 2 LA-ICP-MS

Trace elements abundance was determined by laser ablation inductively coupled plasma mass spectrometry (LA-ICP-MS) using an Agilent 7900 Quadrupole ICP-MS coupled to Resonetics 193 nm laser at the Aarhus Geochemistry and Isotope Research (AGiR) Platform, Aarhus University. Instrumental calibration and tuning are accomplished using the certified reference material NIST 612. Oxides formation was monitored using the $^{248}ThO/^{232}Th$ ratio. A total of 30 masses (^{24}Mg, ^{27}Al, ^{28}Si, ^{48}Ti, ^{53}Cr, ^{55}Mn, ^{57}Fe, ^{59}Co,

^{60}Ni, ^{66}Zn, ^{72}Ge, ^{75}As, ^{77}Se, ^{103}Rh, ^{105}Pd, ^{106}Pd, ^{111}Cd, ^{114}Cd, ^{113}In, ^{115}In, ^{118}Sn, ^{121}Sb, ^{125}Te, ^{128}Te, ^{130}Te, ^{194}Pt, ^{195}Pt, ^{197}Au, ^{206}Pb, ^{209}Bi) were acquired. ^{24}Mg, ^{27}Al, ^{48}Ti, ^{57}Fe, ^{72}Ge, ^{103}Rh, ^{105}Pd, ^{114}Cd and ^{113}In are not considered in the discussion (but are reported in the Supplement 1) due to their polyatomic/isobaric interferences [38,39]. Typically we analysed the core or centre of the sample five times and rim or near surface area three times with a 72 µm laser spot operating at 10 Hz repetition rate, 80 mJ laser energy with 50% attenuated value for a fluence of approximately 5 J/cm^2. Each ablation sequence consisted of 20 sec background acquisition, 35 sec sampling time, and 25 sec washout.

For processing time resolved signal obtained from LA-ICP-MS, a data reduction software IoliteTM was used to inspect and quantify the composition of trace elements. Rare earth elements have background count rates that are mostly zero permitting us to use the calculation scheme of Howell et al. to estimate the limit of detection (LOD) [40]. For quantification and instrumental performance measurement (accuracy and precision), six silver standards from MBH Analytical Ltd. were included in the analysis. Standards 133X AGA1, 133X AGA2, 133X AGA3 are silver-alloy standards, while 131X AGP1, 131X AGP2, 131X AGP3 were pure silver standards. For data reduction in IoliteTM, the time resolved signal was quantified with 133X AGA1, 133X AGA2 and 133X AGA3 using Pb and Ag as internal standards, resulting in six different quantifications. Each standard was analysed five times, from which the median was calculated for every quantification and compared to the reported composition of the standards. The best matched results were selected, which in this case is 133X AGA3 with Ag as the internal standard. Analysis of standards and the analytical reproducibility are reported in Supplement 1.

3. Results and Discussion

3. 1 Silver surface enrichment

3. 1. 1 µXRF

The µXRF analysis showed that coin samples Rom 107, Rom 141, Rom 155, Rom 157, and Sas 2a have a higher content of Ag at the surface than in the core (Table 2). As seen in Figure 2, coins Rom 107, Rom 140, Rom 141, Rom 155, Rom 157 and Sas 2 display different levels of Cu depletion in near-surface areas with varying thicknesses and homogeneity. In the case of Roman denarii; Rom 107, Rom 155 and Rom 157 have discernible enriched zones, while for Rom 140 the distinction is less apparent. The layer is c. 80 µm thick and more abundant in Cu than depleted areas in other coins. Coins Rom 107 and Rom 155 have an even and relatively thick enriched layer, while the thickness of enriched areas in Rom 157 varies from 70 to 550 µm across the near-surface area. Besides enriched areas, elemental mapping of Sas 2 shows the presence of a corrosion layer with a variable thickness. In the case of Rom 141, the elemental map shows almost complete depletion of Cu from the hearth of the coin, with a few Cu corrosion pockets present in the

interior. The enrichment is not limited to the near-surface area as it reaches the core of the coin. The elemental map of Sas 1, Sas 3 and Uma coins do not show traces of enrichment. Ag and Cu are evenly distributed in the near-surface and bulk areas.

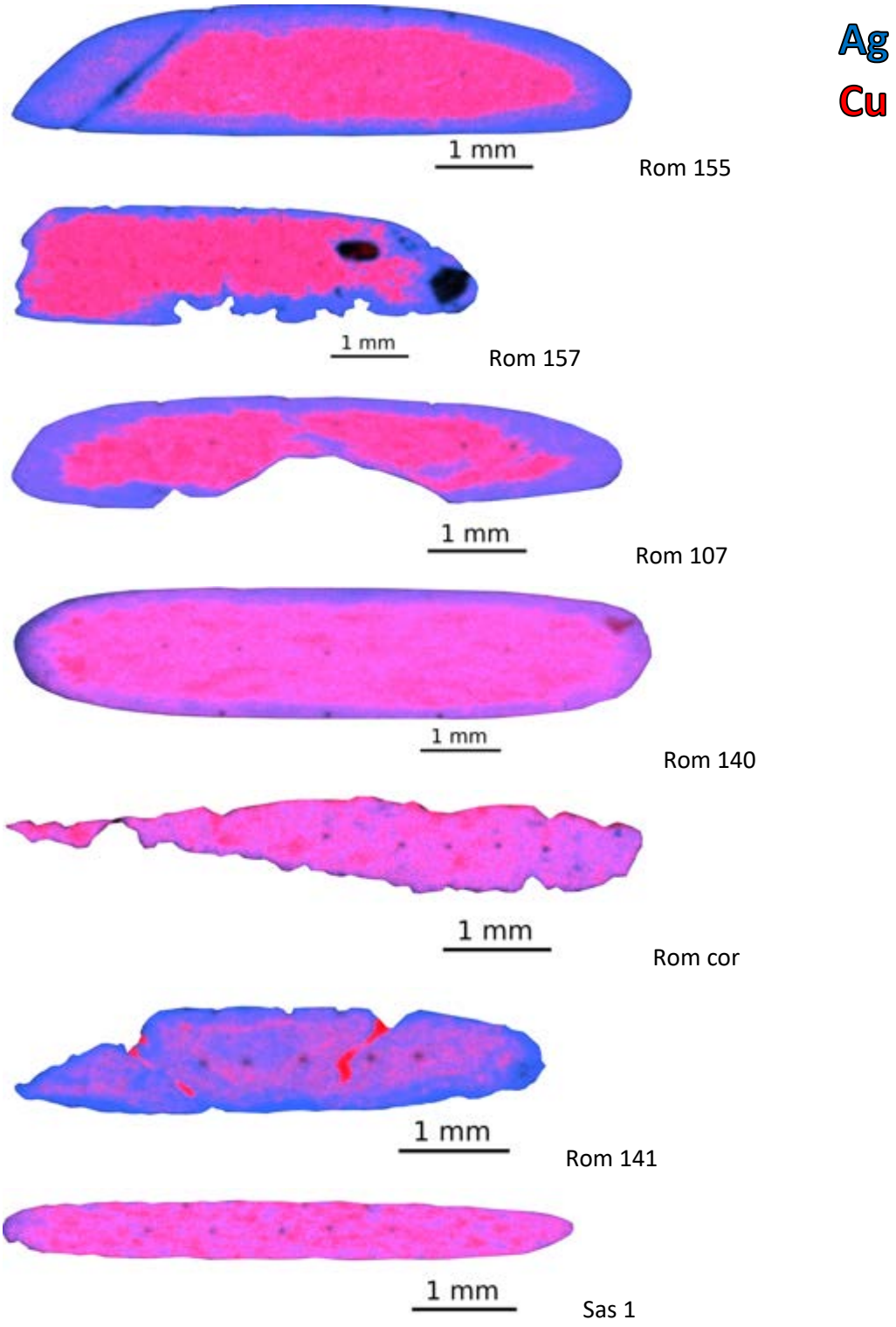

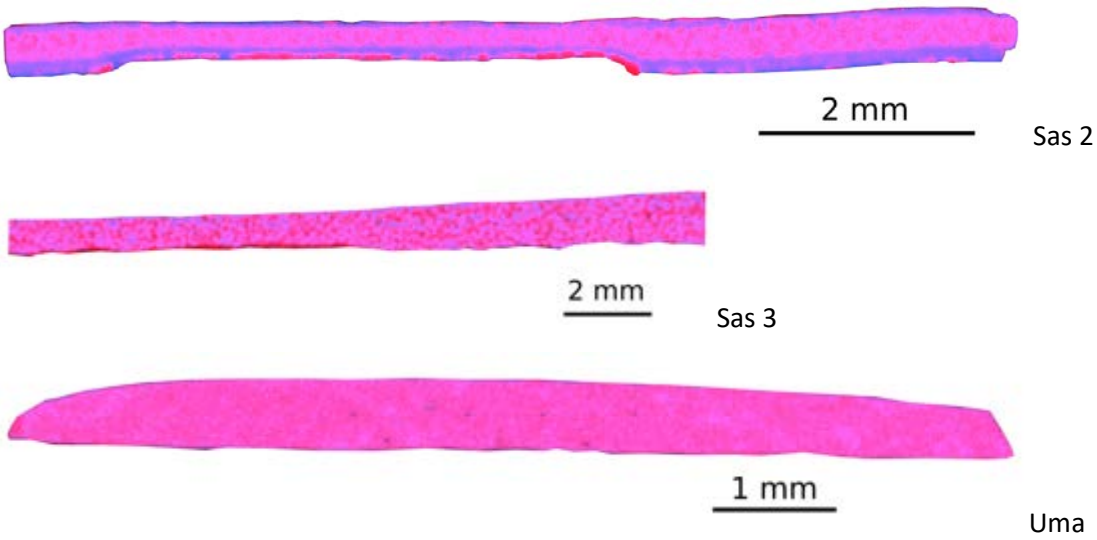

Figure 2 µXRF elemental maps of coin cross-sections showing the distribution of Ag and Cu.

The intensity measurements of Ag Kα and Ag Lα peaks from coins were compared to the Ag Kα/Ag Lα ratio measured from silver-alloy reference materials (RM); coins exhibiting no enriched surface should have similar matrixes and have the same ratio to the most comparable standard. A lower Ag Kα/Ag Lα ratio relative to the standard suggests the presence of a surface enrichment. The difference between ratios of coins and standards are presented as percent deviation in Table 2, while the visual representation of the difference is shown in Figure 3 where coins with enrichment were marked red. The negative percentage deviation suggests the occurrence of surface enrichment on a coin, while a large positive percentage deviation indicates the presence of a corrosion layer. As explained by Linke & Schreiner[13], the difference in intensity ratios between coin's surface and silver standards can be used to assess the degree of depletion or the presence of corrosion layers on the coin's surface. This can be illustrated for sample Rom 140. Here, the surface contains a relatively small enrichment, which is also confirmed with the µXRF results of bulk and surface areas of Rom 140. For all coins with enrichment, the thickness of layers vary, but are relatively well explained by the degree of percentage deviation. However, this should not be extrapolated to predict the theoretical thickness of the enrichment as it mainly refers to the amount of Cu depletion and not to the depth of the layer. A layer of enrichment can be thin, but strongly depleted in Cu. The same can be said in cases where Cu depletion processes occur deeper in a coin, but with a significant amount of Cu still remaining. Factors such as composition, galvanic corrosion or intentional surface treatment have an effect on the amount and depth of Cu depletion [5].

Table 2 The percent deviation of Ag Kα/Ag Lα ratios of different silver coins from the Ag Kα/Ag Lα ratios gathered from non-corroded Ag alloy standards. The table is colour coded to highlight the difference. The gradient scale — red/orange indicate silver surface enrichment (SSE), yellow/pale green show coins where surface and bulk Ag composition do not differ, dark green suggests the presence of a corrosion layer on the surface.

Coin type	Ruler	Abbreviation*	µXRF Ag (wt%)		AgK/AgL	133X AGA1	133X AGA2	133X AGA3	131X AGP1-1
			surface	core					
Roman (107-108 AD)	Traianus (98-117 AD)	Rom 107	95.00	74.85	0.0966	-7.6	-8.2	-4.1	2.4
Roman (103-111 AD)	Traianus (98-117 AD)	Rom 103	93.64	/	0.0993	-5.0	-5.7	-1.4	5.2
Roman (157-158 AD)	Antoninus Pius (138-161 AD)	Rom 157	93.70	68.49	0.1007	-3.6	-4.3	0.0	6.8
Roman (155 AD)	Antoninus Pius (138-161 AD)	Rom 155	94.23	73.25	0.1029	-1.6	-2.2	2.2	9.1
Roman (140-143 AD)	Antoninus Pius (138-161 AD)	Rom 140	94.44	92.81	0.1036	-0.9	-1.5	2.9	9.9
Roman (141 AD)	Antoninus Pius (138-161 AD)	Rom 141	97.33	82.64	0.1092	4.5	3.8	8.4	15.8
Roman (unidentified)	unidentified	Rom cor	94.92	94.21	0.1167	11.6	10.8	15.8	23.7
Sasanian drachma (unknown)	unidentified	Sas 1a	96.37	95.56	0.1132	8.3	7.5	12.4	20.0
		Sas 1b	96.19	95.56	0.1144	9.4	8.7	13.6	21.3
Sasanian drachma (unknown)	unidentified	Sas 2a	91.93	84.41	0.1227	17.4	16.6	21.8	30.1
		Sas 2b	/	84.41	0.1444	38.2	37.2	43.4	53.1
Sasanian drachma (unknown)	unidentified	Sas 3a	95.59	95.40	0.1431	36.9	36.0	42.1	51.7
		Sas 3b	95.70	95.40	0.1339	28.1	27.2	33.0	42.0
Umayyad dirham (95 AH/713 AD), Dārābjird,	Al-Walid I (86-105 AH/705-723AD)	Uma a	93.35	93.83	0.1163	11.2	10.4	15.4	23.2
		Uma b	94.19	93.83	0.1141	9.1	8.4	13.2	20.9
Abbasid dirham (187 AH/803 AD), Madīnat as-Salām,	Harun al-Rashid (170-193 AH/786-809 AD)	Abb a	98.18	/	0.1124	7.5	6.8	11.6	19.2
		Abb b	98.16	/	0.1115	6.7	5.9	10.7	18.2

* a = obverse, b = reverse

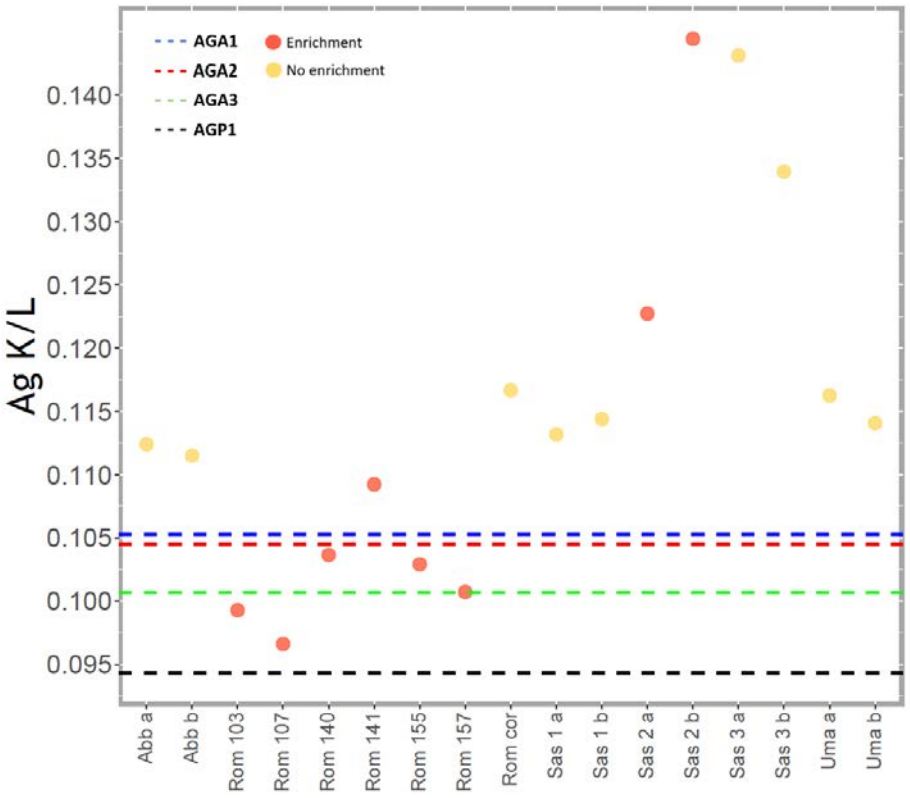

Figure 3 Ag Kα/Ag Lα ratios of silver coins for this study compared to ratios obtained for the silver standards. Coins for which the surface enrichment is confirmed in the cross-section analysis are shown in red.

As mentioned previously, measuring the Ag Kα/Ag Lα ratios require comparison to standards of similar composition and matrix. Even though the coins analysed are different when it comes to the provenance, the µXRF analysis of the coin surfaces suggest all coins to be very or extra fine by the European grading system. Comparing intensity ratios show that the identification of surface enrichment in coins depends on the standard with which they are compared. When coins were compared to 133X AGA1 and 133X AGA2 standards, 5 Roman denarii had a lower ratio value and percentage deviation, indicating the presence of surface enrichment (Figure 3 and Table 2). The enrichment was not detected in coins Rom 141 and Sas 2. In Rom 141, the depletion of Cu through enrichment and corrosion is thicker than the theoretical XRF information depth, while Sas 2 has a much larger ratio value due to the presence of corrosion. 133X AGA1 and 133X AGA2 can be considered to be very fine in terms of Ag content, but still less pure than 133X AGA3 and 131X AGP1. With 133X AGA3 enrichment was detected only for Rom 103 and Rom 107. 131X AGP1 is an extremely fine standard, and in this group, none of the values indicate the presence of surface enrichment. Early Islamic coins (Uma and Abb) do not deviate significantly from the Ag Kα/Ag Lα ratios

obtained from standards. Sas 2 and Sas3 have a larger positive deviation that suggests the presence of a corrosion layer, which is also visually discernible.

The presence of corrosion in a coin can prevent the XRF analysis from acquiring accurate peak intensity values. Cu will separate from the Ag matrix during enrichment and form corrosion products on the surface. Corrosion layers formed from the segregated Cu will affect the energy signal of Ag secondary radiation, especially L-lines [41]. As seen in Figure 4, by measuring the intensity of Cu Kα and Cu Lα peaks and combining them with Ag lines, it is possible to account for the influence of Cu corrosion products in the spectrum. The information depth of Cu lines attenuates with the increase of Ag content in an Ag-Cu alloy. For Cu Kα radiation (energy 8.04 keV) the information depth in an 80 wt. % Ag – 20 wt. % Cu matrix is approximately 16 μm [18]. In Figure 4 the Cu Kα/Ag Kα ratios are plotted together with Cu Lα/Ag Lα values taken from coins and standards. Standards form a regression line with a high coefficient of determination (R^2 = 0.9998). Coins that exhibit surface enrichment are positioned below the regression line, while the ones without enrichment lie above the line. In the case of Rom 141, the enrichment is larger than the information depth of Ag secondary radiation. Likewise, examination of Sas 2 in cross-section confirms near-surface enrichment; however, due to the corrosion present on the surface, it was not possible to accurately measure Ag Kα/Ag Lα ratio. For Sas 2b, it was possible to identify the surface enrichment despite the presence of corrosion by adding intensity peaks of Cu lines to Ag lines. On the other hand, Sas 2a is positioned above the regression line. As the corrosion thickness appears similar on the both sides of the coins, it is likely that besides Cu corrosion products surface also contains significant amounts of Ag_2S that would influence the energy intensity detected from Ag lines.

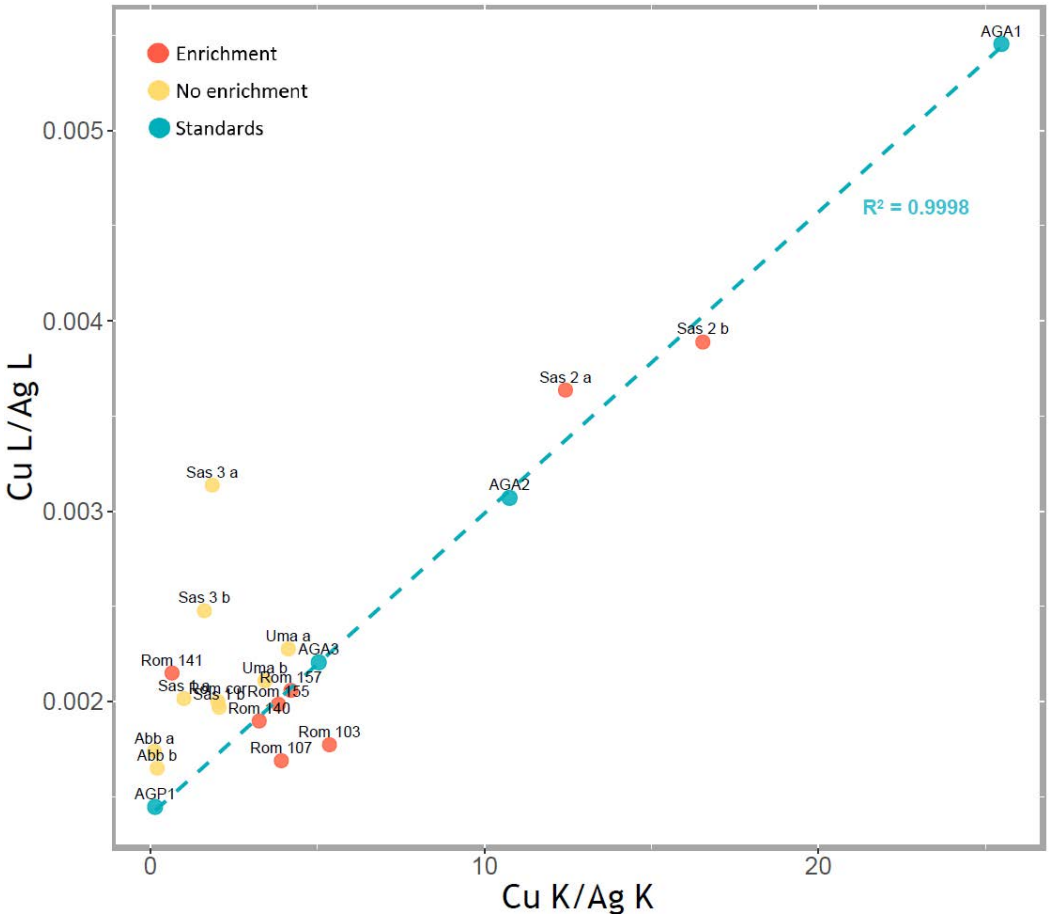

Figure 4 A biplot of Cu Kα/Ag Kα and Cu Lα/Ag Lα ratios obtained from coins and standards. Coin with no enrichment plot above the regression line, while most of the coins with enrichment are positioned below.

3. 2 Trace element behaviour

3. 2. 1 LA-ICP-MS

The result from the centre and rim of sample profile were compared by displaying the abundance of individual elements per coin (Figure 3). The results of four coins that exhibit SSE are presented (Rom 107, Rom 140, Rom 155, Rom 157), while the results of the analysis can be found in Supplement 1.

In his study of SSE in 16th century Portuguese silver coins, Borges et al. [9] conducted elemental depth profiling with LA-ICP-MS with the purpose of studying the superficial Cu depleted level present at a greater depth. The study also reported the difference in the behaviour of minor and trace elements (Au, Pb, Bi, Hg) from a larger depth in the coins. In the case of three coins, Au content decreased with increasing depth, whereas in a Roman denarii, the enriched layer was so substantial that depth profiling might not have reached the unaffected core of a coin. Ablation of the core and the surface allows for a more reliable comparison of quantitative changed in minor and trace elements.

The most relevant trace elements for studying the provenance of silver are Au and Bi. These derive from argentiferous ores from which silver was originally extracted. The behaviour of the elements during smelting, cupellation and melting are discussed elsewhere [23,35]. The LA-ICP-MS analysis shows that Au content substantially increases in the Ag enriched areas. Such behaviour is also noticed even in when the amount of Au is ~280 ppm. Rom 155 contains the largest amount of Au in the group. The Au amount in the enriched layers is larger by a factor of 2 when compared to the core. Due to the almost identical radii, Au and Ag form complete solid solution, while Ag and Cu have a considerable miscibility gap [42].

Bi shows relatively little difference between the core and zone of enrichment in two coins — Rom 140 and Rom 157. In Rom 157, one point has a noticeably higher amount of Bi on the surface. However, this could be due to a heterogeneous distribution of Bi in the Ag alloy. A similar behaviour is seen in Pb, with a similar jump in quantity in the coin Rom 157. Another element commonly detected in Ag-Cu coins is Zn. Only in Rom 140 was it possible to notice significant difference between the core and the rim composition of coins. In the other coins analysed, a significant difference in Zn could not be detected between the surface and the core.

Other trace elements affected by surface enrichment include Co, Ni and As, which are all depleted towards the coin surface relative to core. Co, Ni and As are common tracers in Cu ores and only associated with silver ores if Ag was extracted from cerargyrite (AgCl) or argentite (Ag_2S). In the enrichment process, they follow Cu as these decrease within the enriched areas. Platinum (Pt) is also depleted in the enriched areas, similar to the Cu group trace elements. A previous study of trace elements in silver coins have suggested a possible correlation between Ag and Pt [43], whereas Pernicka [44] relates platinum group metals (PGE) to the presence of alluvial Au. Pernicka attributes the PGEs in silver to cases where silver was separated from high Ag native gold coming from alluvial deposits through the process of cementation [44]. However, in the coins analysed here, Au and Pt have a negative correlation suggesting that Pt was depleted from the surface together with Cu. Further studies are necessary to fully explore the relationship between Au and Pt in historical silver objects.

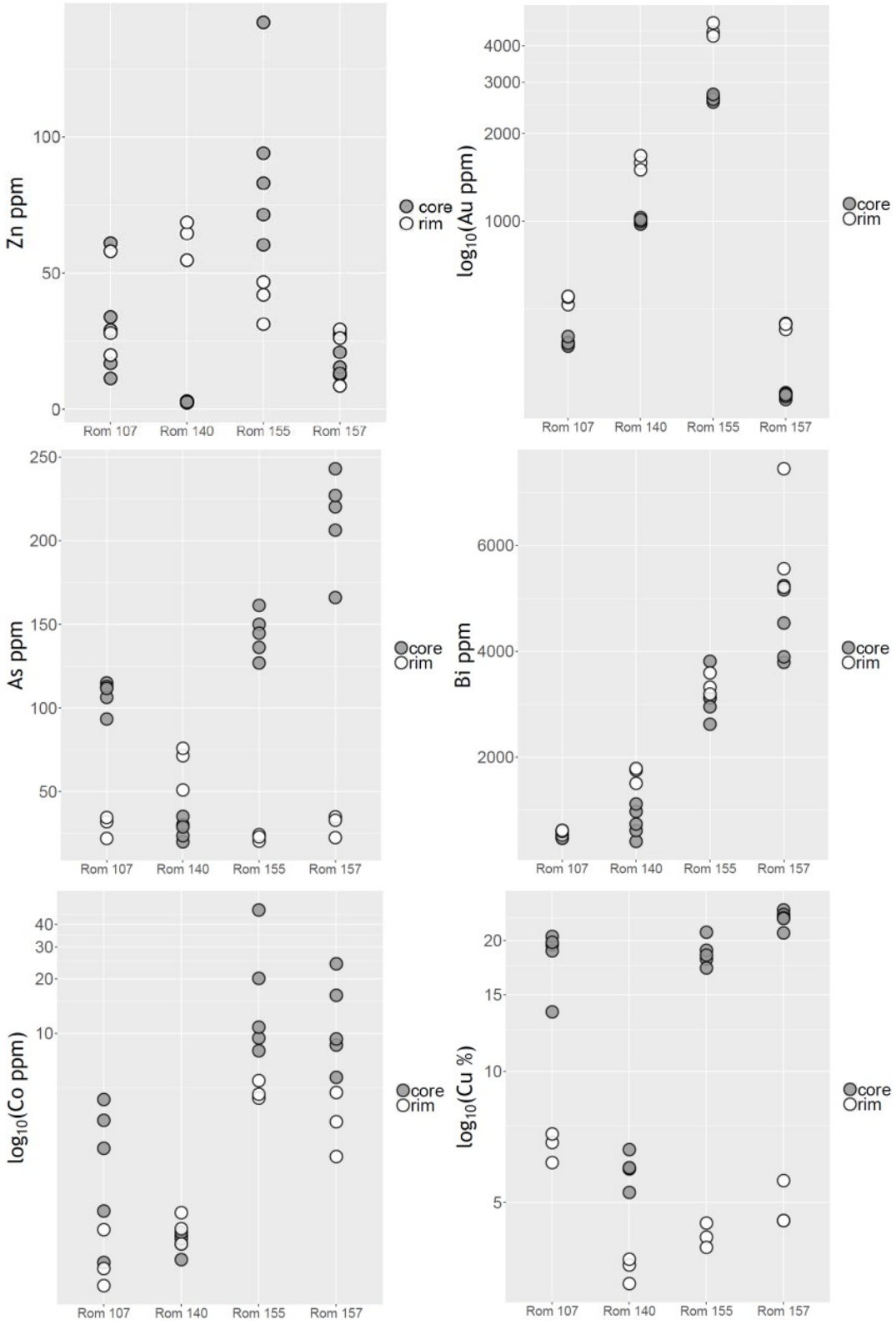
Zn ppm
100
50
0
Rom 107
Rom 140
Rom 155
Rom 157
core
rim
log10(Au ppm)
4000
3000
2000
1000
As ppm
250
200
150
100
50
Bi ppm
6000
4000
2000
log10(Co ppm)
40
30
20
10
log10(Cu %)
20
15
10
5

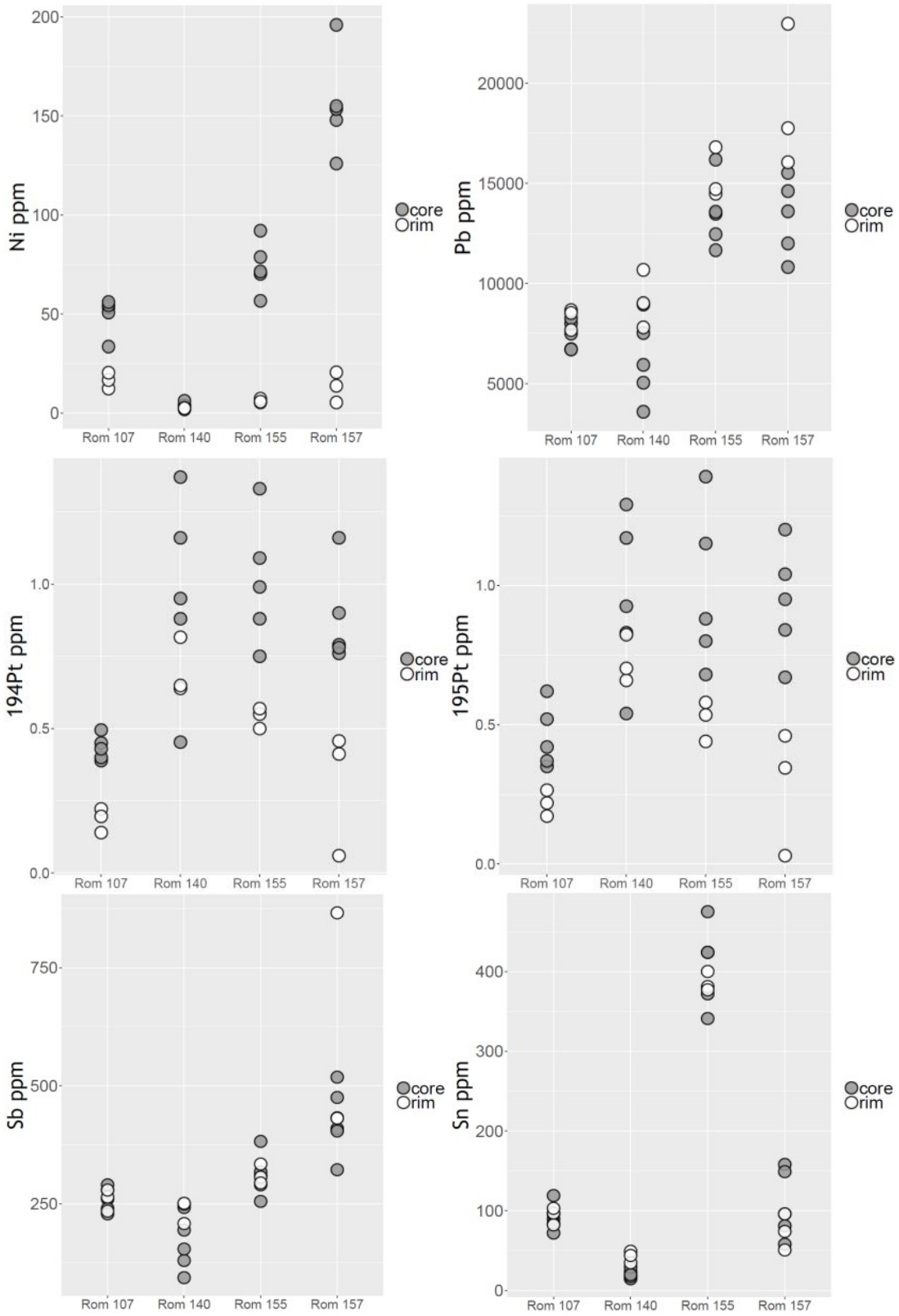

Figure 3 Comparison of the composition of minor and trace elements between the core and the rim of enriched coins.

4. Conclusion

Non-destructive identification of silver surface enrichment was successfully confirmed through the Ag Kα/Ag Lα intensity ratio comparison. As reported in previous studies, the deviation is indicative of the amount of Cu depletion rather than the thickness of enriched areas. We show that the choice of standard is critical for correctly determining surface enrichment when measuring Ag Kα/Ag Lα peak ratios. In the cases of surface screening a large number of Ag-Cu coins, the researcher or conservator should consider the compositional heterogeneity of the coins and ideally use multiple standards for assessing the surface enrichment. The Ag alloy standards must have original composition of the studied coins. For the Roman coins studied here, we show Ag contents to differ by up to 50 % for the core relative to the enriched surface. Thus, by considering standards with a range in Ag and Cu concentrations, it is possible to account for the compositional discrepancy between the surface and the core of unknown coins. In enriched coins where corrosion is present on the surface, combining Ag lines with the values obtained from Cu Kα and Cu Lα can be used to identify the surface enrichment below the corrosion layer.

Besides Ag and Cu, surface enrichment also affects minor and trace elements such as e.g. Au, which may be enriched by a factor of 2 at the enriched surface. This can result in an overestimation of Au and be misleading for silver provenance interpretations if based on analytical results from the surface. The study did not detect significant differences in Pb, Bi and Zn concentrations at surface versus core, whereas trace elements such as Co, Ni and As show depletion in enriched areas. As these elements are mainly associated with Cu and Cu ores, it is suggested that most likely they are leached together with Cu from the surface.

The effect of enrichment not only affects Ag and Cu concentrations, but also the concentration of important trace element Au. Identifying coins that exhibit such behaviour is therefore not only critical for studying aspects of past economies such as fineness and debasement, but also for provenance interpretations. A multi-standard approach allows researchers to circumvent this issue by identifying the coins where enrichment is present, thus influencing their final coin selections for analytical investigations.

Acknowledgment

This work was supported by the Danish National Research Foundation under the grant DNRF119 – Centre of Excellence for Urban Network Evolutions (UrbNet). The authors would like to thank Michael Blömer for identifying the Roman coins.

Literature

[1] T. Birch, K.J. Westner, F. Kemmers, S. Klein, H.E. Höfer, H. -M. Seitz, Retracing Magna Graecia's silver: coupling lead isotopes with a multi-standard trace element procedure, Archaeometry. 62 (2020) 81–108. https://doi.org/10.1111/arcm.12499.

[2] K. Butcher, M. Ponting, The Metallurgy of Roman Silver Coinage: From the Reform of Nero to the Reform of Trajan, Cambridge, United Kingdom: Cambridge University Press, 2015.

[3] E. Pernicka, Erzlagerstätten in der Ägäis und ihre Ausbeutung im Altertum: geochemische Untersuchungen zur Herkunftsbestimmung archäologischer Metallobjekte, Jahrb. Röm.-Ger. Zentralmuseum. 34 (1987) 607–720.

[4] F.J. Ager, A.I. Moreno-Suárez, S. Scrivano, I. Ortega-Feliu, B. Gómez-Tubío, M.A. Respaldiza, Silver surface enrichment in ancient coins studied by micro-PIXE, Nucl. Instrum. Methods Phys. Res. Sect. B Beam Interact. Mater. At. 306 (2013) 241–244. https://doi.org/10.1016/j.nimb.2012.12.037.

[5] L. Beck, E. Alloin, C. Berthier, S. Réveillon, V. Costa, Silver surface enrichment controlled by simultaneous RBS for reliable PIXE analysis of ancient coins, Nucl. Instrum. Methods Phys. Res. Sect. B Beam Interact. Mater. At. 266 (2008) 2320–2324. https://doi.org/10.1016/j.nimb.2008.03.084.

[6] L. Beck, S. Bosonnet, S. Réveillon, D. Eliot, F. Pilon, Silver surface enrichment of silver–copper alloys: a limitation for the analysis of ancient silver coins by surface techniques, Nucl. Instrum. Methods Phys. Res. Sect. B Beam Interact. Mater. At. 226 (2004) 153–162. https://doi.org/10.1016/j.nimb.2004.06.044.

[7] L. Cope, Surface-silvered Ancient Coins, in: E.T. Hall, D.M. Metcalf (Eds.), Methods Chem. Metall. Investig. Anc. Coin., Royal Numismatic Society, London, 1972: pp. 261–278.

[8] C. Flament, P. Marchetti, Analysis of ancient silver coins, Nucl. Instrum. Methods Phys. Res. Sect. B Beam Interact. Mater. At. 226 (2004) 179–184. https://doi.org/10.1016/j.nimb.2004.03.078.

[9] R. Borges, L. Alves, R.J.C. Silva, M.F. Araújo, A. Candeias, V. Corregidor, P. Valério, P. Barrulas, Investigation of surface silver enrichment in ancient high silver alloys by PIXE, EDXRF, LA-ICP-MS and SEM-EDS, Microchem. J. 131 (2017) 103–111. https://doi.org/10.1016/j.microc.2016.12.002.

[10] E.T. Hall, Surface-enrichment of buried metals, Archaeometry. 4 (1961) 62–66. https://doi.org/10.1111/j.1475-4754.1961.tb00535.x.

[11] G. Sarah, B. Gratuze, J.-N. Barrandon, Application of laser ablation inductively coupled plasma mass spectrometry (LA-ICP-MS) for the investigation of ancient silver coins, J. Anal. At. Spectrom. 22 (2007) 1163. https://doi.org/10.1039/b704879c.

[12] R. Klockenkämper, H. Bubert, K. Hasler, Detection of near-surface silver enrichment on Roman imperial silver coins by X-ray spectral analysis, Archaeometry. 41 (1999) 311–320. https://doi.org/10.1111/j.1475-4754.1999.tb00985.x.

[13] R. Linke, M. Schreiner, Energy Dispersive X-Ray Fluorescence Analysis and X-Ray Microanalysis of Medieval Silver Coins, Microchim. Acta. 133 (2000) 165–170. https://doi.org/10.1007/s006040070087.

[14] A. Deraisme, L. Beck, F. Pilon, J.N. Barrandon, A study of the silvering process of the Gallo-Roman coins forged during the thrid century AD, Archaeometry. 48 (2006) 469–480.

[15] C. Vlachou, J.G. McDonnell, R.C. Janaway, Experimental investigation of silvering in late Roman coinage, MRS Proc. 712 (2002). https://doi.org/10.1557/PROC-712-II9.2.

[16] H. Gitler, M. Ponting, Rome and the East: A Study of the Chemical Composition of Roman Silver Coinage During the Reign of Septimius Severus 193-211 AD, in: Proc. Colloq.

Prod. Échanges Dans Syr. Gréco-Romaine Tours June 12-13, Topoi. suppl. 8, 2003: pp. 375–397.
[17] C.N. Zwicky-Sobczyk, W.B. Stern, X-ray flourescence and density measurments on surface-treated Roman Silver Coins, Archaeometry. 39 (1997) 393–405. https://doi.org/10.1111/j.1475-4754.1997.tb00815.x.
[18] R. Linke, M. Schreiner, G. Demortier, M. Alram, Determination of the provenance of medieval silver coins: potential and limitations of x-ray analysis using photons, electrons or protons, X-Ray Spectrom. 32 (2003) 373–380. https://doi.org/10.1002/xrs.654.
[19] R. Linke, M. Schreiner, G. Demortier, The application of photon, electron and proton induced X-ray analysis for the identification and characterisation of medieval silver coins, Nucl. Instrum. Methods Phys. Res. Sect. B Beam Interact. Mater. At. 226 (2004) 172–178. https://doi.org/10.1016/j.nimb.2004.03.084.
[20] R. Linke, M. Schreiner, G. Demortier, M. Alram, H. Winter, The provenance of medieval silver coins: analysis with EDXRF, SEMIEDX and PIXE, in: K. Janssens, R. Van Grieken (Eds.), Compr. Anal. Chem. CLII, Elsevier B. V., 2004: pp. 605–633.
[21] F.P. Romano, S. Garraffo, L. Pappalardo, F. Rizzo, In situ investigation of the surface silvering of late Roman coins by combined use of high energy broad-beam and low energy micro-beam X-ray fluorescence techniques, Spectrochim. Acta Part B At. Spectrosc. 73 (2012) 13–19. https://doi.org/10.1016/j.sab.2012.05.012.
[22] R.J. Rosenberg, Determination of the silver content of ancient silver coins by neutron activation analysis, J. Radioanal. Nucl. Chem. Artic. 92 (1985) 171–176. https://doi.org/10.1007/BF02065400.
[23] P. Meyers, E.V. Sayre, The Determination of Trace Elements in Ancient Silver Objects by Thermal Neutron Activation Analysis, Bull. Am. Group Int. Inst. Conserv. Hist. Artist. Works. 11 (1971) 29. https://doi.org/10.2307/3178894.
[24] A. Giumlia-Mair, On surface analysis and archaeometallurgy, Nucl. Instrum. Methods Phys. Res. Sect. B Beam Interact. Mater. At. 239 (2005) 35–43. https://doi.org/10.1016/j.nimb.2005.06.178.
[25] M. Mantler, M. Schreiner, X-ray fluorescence spectrometry in art and archaeology, X-Ray Spectrom. 29 (2000) 3–17. https://doi.org/10.1002/(SICI)1097-4539(200001/02)29:1<3::AID-XRS398>3.0.CO;2-O.
[26] J. Lekki, M. Matosz, C. Paluszkiewicz, E. Pięta, T. Pieprzyca, Z. Szklarz, J.M. del Hoyo Meléndez, Comparison of PIXE and XRF in the analysis of silver denarii of the early Piast, J. Radioanal. Nucl. Chem. 314 (2017) 2309–2316. https://doi.org/10.1007/s10967-017-5556-8.
[27] Zs. Kasztovszky, E. Panczyk, W. Fedorowicz, Zs. Révay, Comparative archaeometrical study of Roman silver coins by prompt gamma activation analysis and SEM-EDX, J. Radioanal. Nucl. Chem. 265 (2005) 193–199. https://doi.org/10.1007/s10967-005-0809-3.
[28] M. Haschke, Laboratory Micro-X-Ray Fluorescence Spectroscopy, Springer International Publishing, Cham, 2014. https://doi.org/10.1007/978-3-319-04864-2.
[29] W.B. Stern, On Non-Destructive Analysis of Gold Objects, in: G. Morteani, J.P. Northover (Eds.), Prehist. Gold Eur., Springer Netherlands, Dordrecht, 1995: pp. 317–328. https://doi.org/10.1007/978-94-015-1292-3_20.
[30] J.M. del Hoyo-Meléndez, P. Świt, M. Matosz, M. Woźniak, A. Klisińska-Kopacz, Ł. Bratasz, Micro-XRF analysis of silver coins from medieval Poland, Nucl. Instrum. Methods Phys. Res. Sect. B Beam Interact. Mater. At. 349 (2015) 6–16. https://doi.org/10.1016/j.nimb.2015.02.018.

[31] R. Lehmann, Archäometallurgie von mittelalterlichen deutschen Silberbarren und Münzen, PhD Thesis, Universität Hannover, 2011.
[32] E. Pernicka, Possibilities and limitations of provenance studies of ancient silver and gold, in: H. Meller, R. Risch, E. Pernicka (Eds.), Met. Macht – Frühes Gold Silber 6 Mitteldtsch. Archäol. Vom 17 Bis 19 Oktober 2013 Halle Saale, 2014: pp. 153–164.
[33] T. Birch, K.J. Westner, F. Kemmers, S. Klein, H.E. Höfer, H. -M. Seitz, Retracing Magna Graecia's silver: coupling lead isotopes with a multi-standard trace element procedure, Archaeometry. (2019) arcm.12499. https://doi.org/10.1111/arcm.12499.
[34] M. L'Héritier, S. Baron, L. Cassayre, F. Téreygeol, Bismuth behaviour during ancient processes of silver–lead production, J. Archaeol. Sci. 57 (2015) 56–68. https://doi.org/10.1016/j.jas.2015.02.002.
[35] E. Pernicka, H.-G. Bachmann, Archäometallurgische Untersuchungen zur antiken Silbergewinnung in Laurion, na, 1983.
[36] P. Meyers, L. Van Zelst, E.V. Sayre, Major and Trace Elements in Sasanian Silver, in: C.W. Beck (Ed.), Archaeol. Chem., AMERICAN CHEMICAL SOCIETY, WASHINGTON, D. C., 1974: pp. 22–33. https://doi.org/10.1021/ba-1974-0138.ch003.
[37] L. Ilisch, F. Schwarz, Die Analysen der Islamischen Münzen, in: L. Ilisch, S. Lorenz, W.B. Stern, H. Steuer (Eds.), Dirham Rappenpfennig Mittelalt. Münzprägung Bergbauregionen Z. Für Archäol. Mittelalt., Bonn, 2003: pp. 51–115.
[38] R. Thomas, A Beginner's Guide to ICP-MS, (n.d.) 8.
[39] T.W. May, R.H. Wiedmeyer, A table of polyatomic interferences in ICP-MS, At. Spectrosc. 19 (1998) 150–155.
[40] D. Howell, W.L. Griffin, N.J. Pearson, W. Powell, P. Wieland, S.Y. O'Reilly, Trace element partitioning in mixed-habit diamonds, Chem. Geol. 355 (2013) 134–143. https://doi.org/10.1016/j.chemgeo.2013.07.013.
[41] M. Ferretti, The investigation of ancient metal artefacts by portable X-ray fluorescence devices, J Anal Spectrom. 29 (2014) 1753–1766. https://doi.org/10.1039/C4JA00107A.
[42] J.C. Kraut, W.B. Stern, The density of gold-silver-copper alloys and its calculation from the chemical composition, Gold Bull. 33 (2000) 52–55. https://doi.org/10.1007/BF03216580.
[43] S. Merkel, Silver and the silver economy at Hedeby, VML Verlag Marie Leidorf, Bochum, 2016.
[44] E. Pernicka, Provenance and recycling of ancient silver. A comment on "Iridium to provenance ancient silver" by Jonathan R. Wood, Michael F. Charlton, Mercedes Murillo-Barroso, Marcos Martinón-Torres. J. Archaeol. Sci. 81, 1–12, J. Archaeol. Sci. 86 (2017) 123–126. https://doi.org/10.1016/j.jas.2017.07.004.